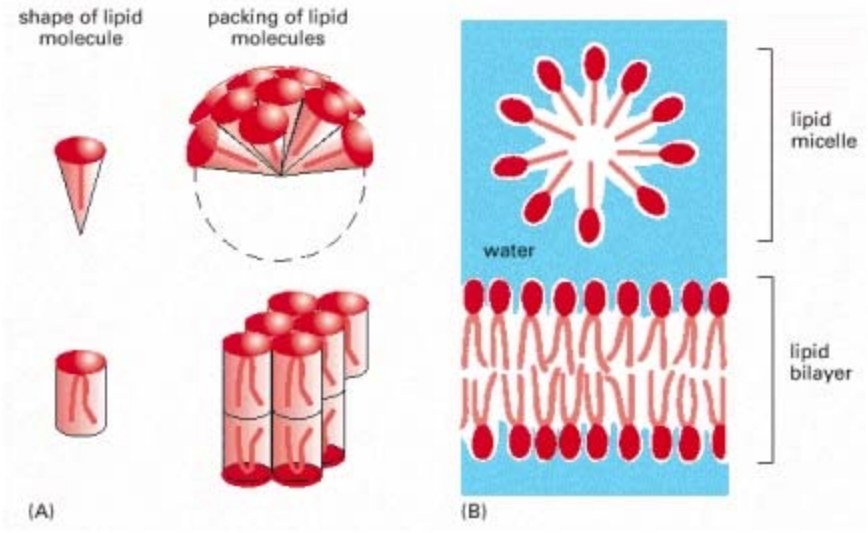

Figure 10-4

. **Packing arrangements of lipid molecules in an aqueous environment**

(A) Wedge-shaped lipid molecules *(above)* form micelles, whereas cylinder-shaped phospholipid molecules *(below)* form bilayers. (B) A lipid micelle and a lipid bilayer seen in cross section. Lipid molecules spontaneously form one or other of these structures in water, depending on their shape.

http://www.ncbi.nlm.nih.gov/bookshelf/br.fcgi?book=mboc4&part=A1864&rendertype=figure&id=A1868

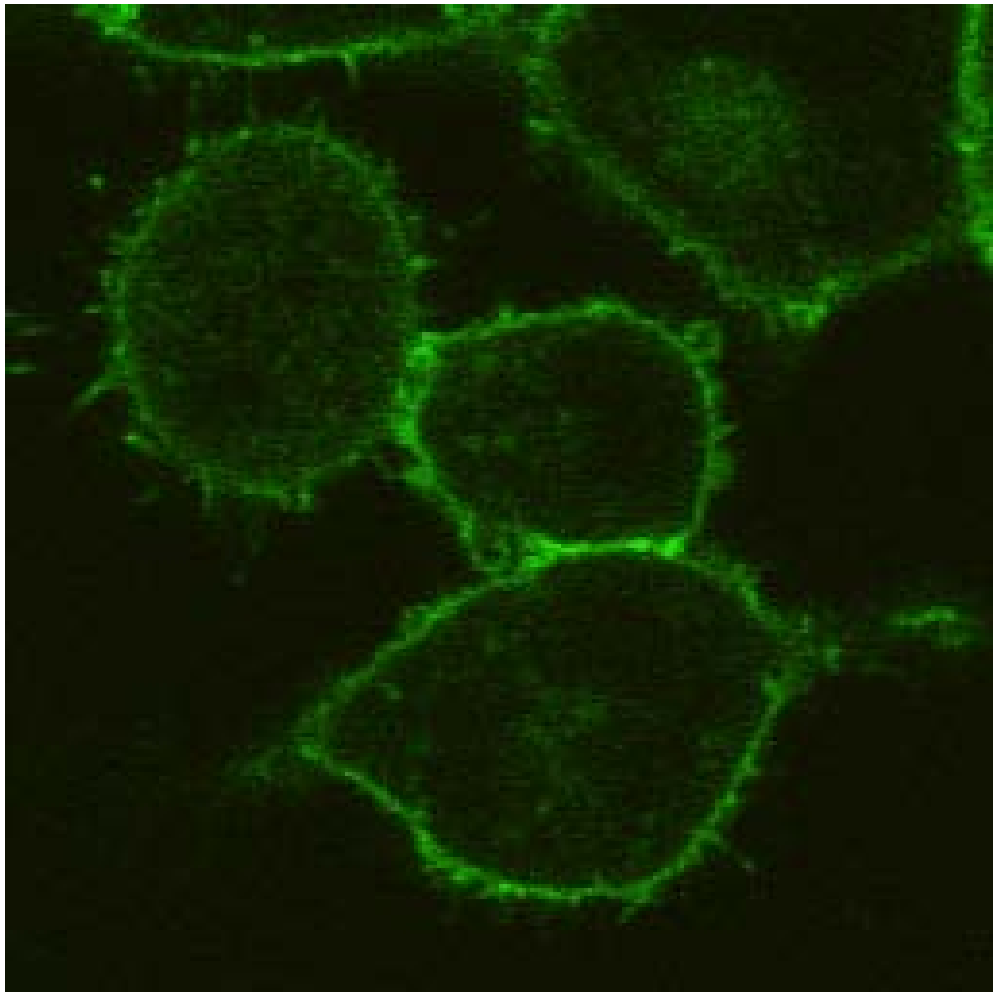

A confocal microscope image of cells transfected with a fluorescent, transmembrane protein

COMMON FATTY ACIDS

These are carboxylic acids with long hydrocarbon tails.

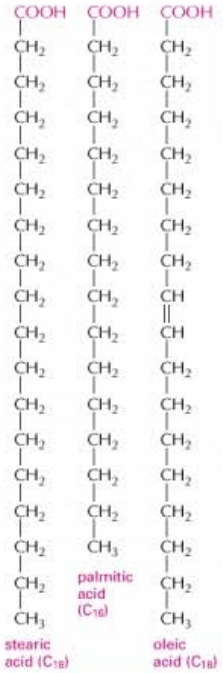

TRIACYLGLYCEROLS

Fatty acids are stored as an energy reserve (fats and oils) through an ester linkage to glycerol to form triacylglycerols, also known as triglycerides.

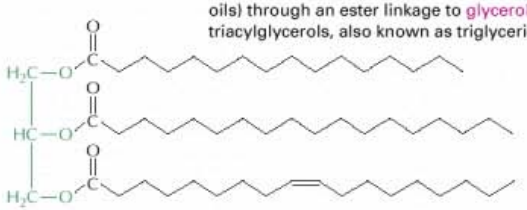

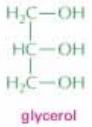

Hundreds of different kinds of fatty acids exist. Some have one or more double bonds in their hydrocarbon tail and are said to be unsaturated. Fatty acids with no double bonds are saturated.

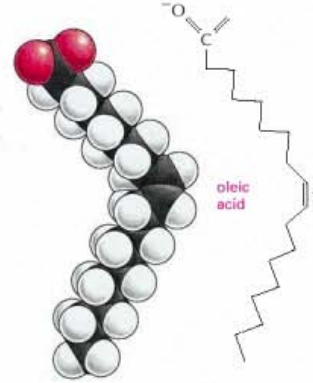

This double bond is rigid and creates a kink in the chain. The rest of the chain is free to rotate about the other C–C bonds.

UNSATURATED

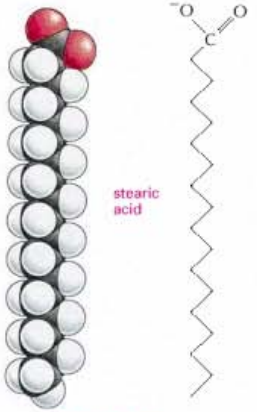

SATURATED

CARBOXYL GROUP

If free, the carboxyl group of a fatty acid will be ionized.

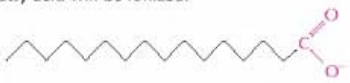

But more usually it is linked to other groups to form either esters

or amides.

PHOSPHOLIPIDS

Phospholipids are the major constituents of cell membranes.

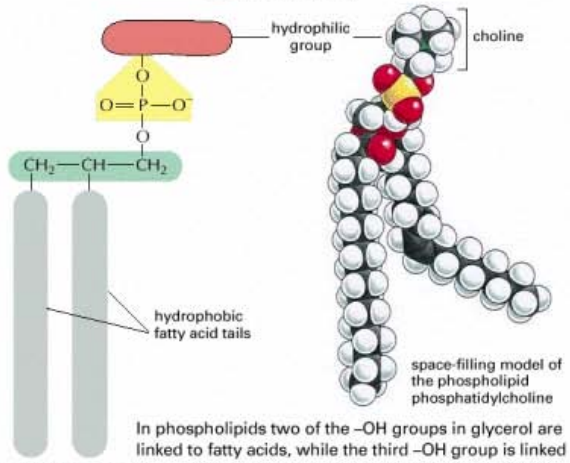

In phospholipids two of the –OH groups in glycerol are linked to fatty acids, while the third –OH group is linked to phosphoric acid. The phosphate is further linked to one of a variety of small polar groups (alcohols).

http://www.ncbi.nlm.nih.gov/bookshelf/br.fcgi?book=mboc4&part=A165&rendertype=box&id=A210

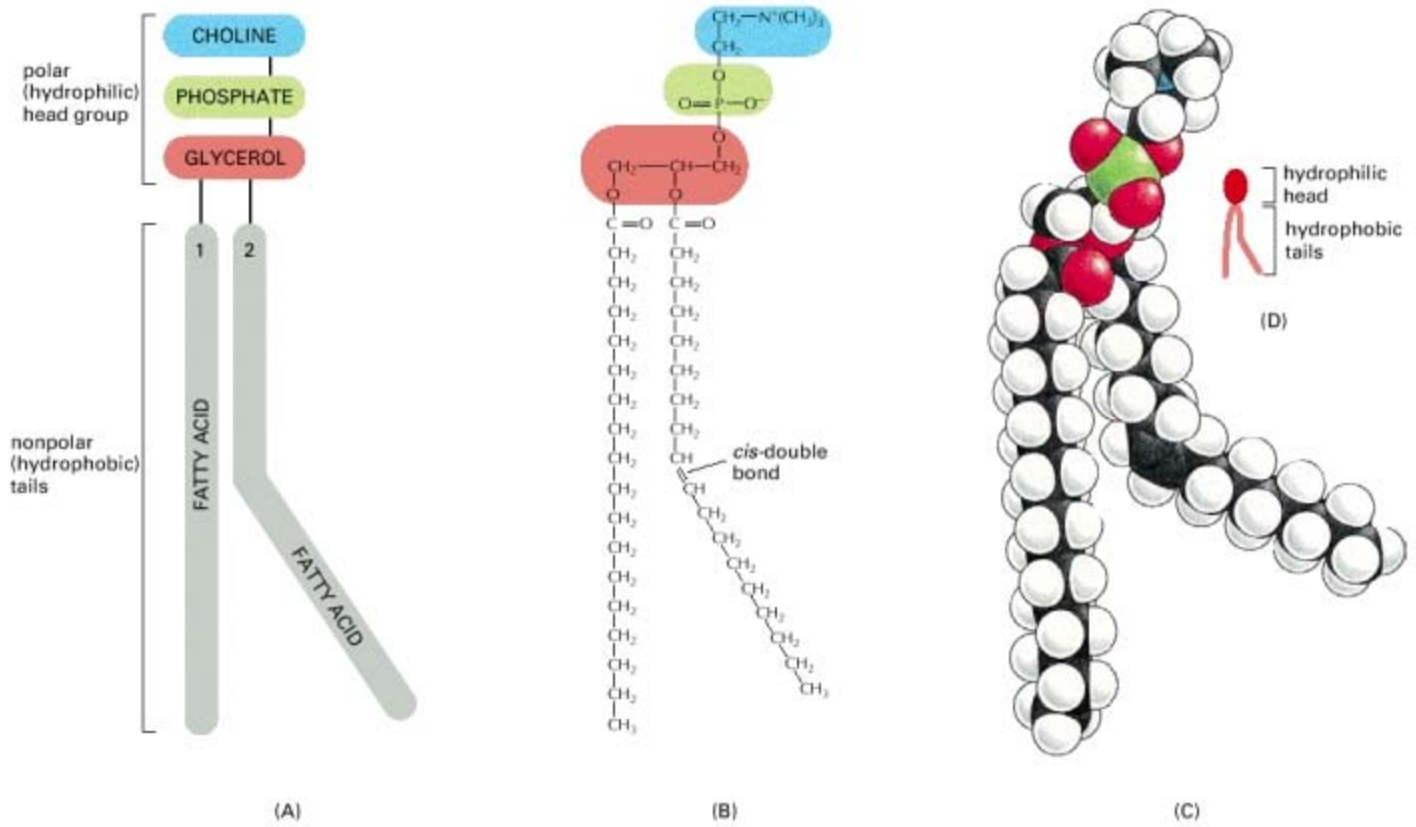

Figure 10-2

. **The parts of a phospholipid molecule**

This example is phosphatidylcholine, represented (A) schematically, (B) by a formula, (C) as a space-filling model, and (D) as a symbol. The kink resulting from the *cis*-double bond is exaggerated for emphasis.

http://www.ncbi.nlm.nih.gov/bookshelf/br.fcgi?book=mboc4&part=A1864&rendertype=figure&id=A1866

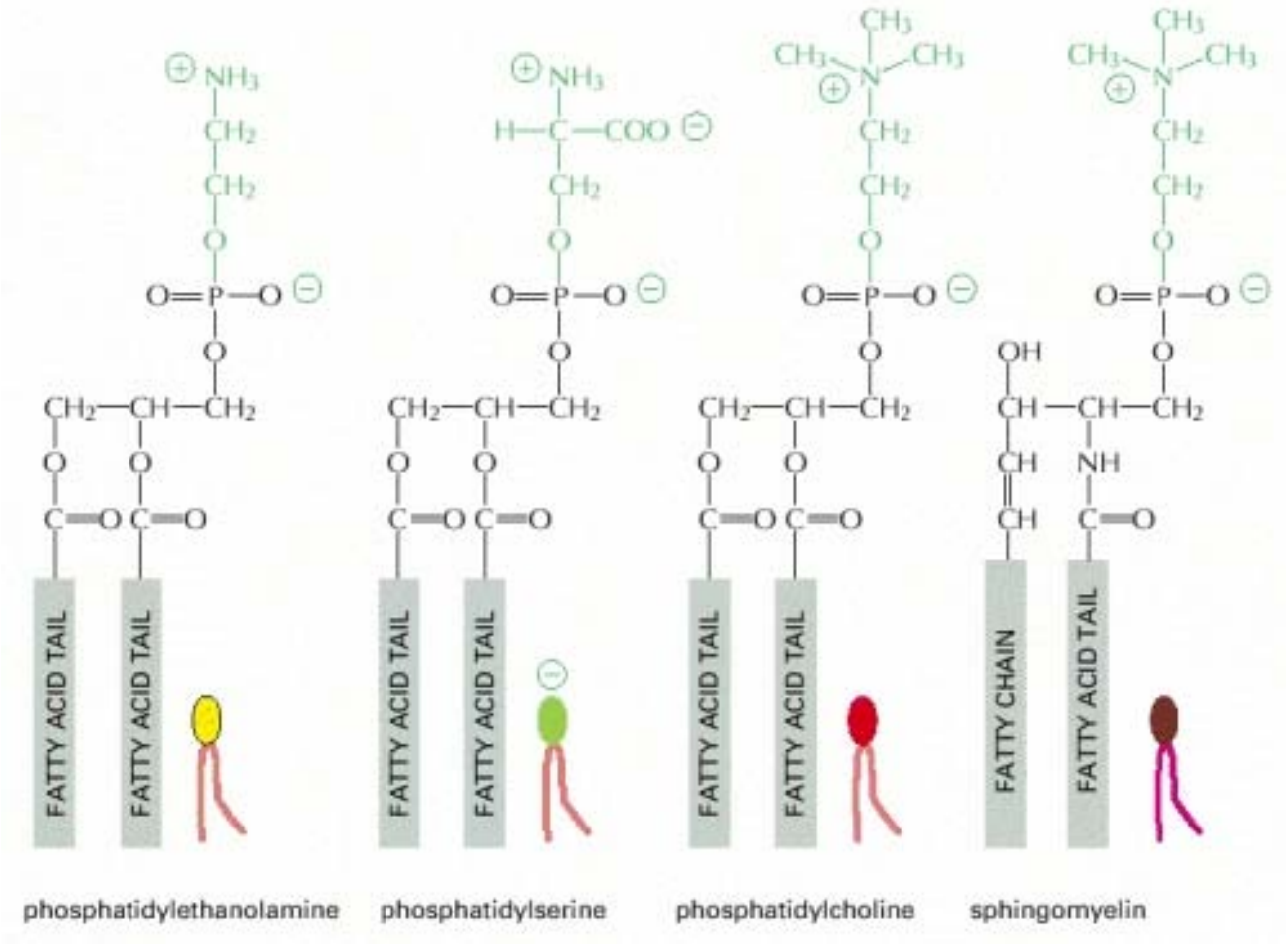

Figure 10-12

. **Four major phospholipids in mammalian plasma membranes**

Note that different head groups are represented by different colors. All the lipid molecules shown are derived from glycerol except for sphingomyelin, which is derived from serine.

http://www.ncbi.nlm.nih.gov/bookshelf/br.fcgi?book=mboc4&part=A1864&rendertype=figure&id=A1879

	PERCENTAGE OF TOTAL LIPID BY WEIGHT					
LIPID	LIVER CELL PLASMA MEMBRANE	RED BLOOD CELL PLASMA MEMBRANE	MYELIN	MITOCHONDRION (INNER AND OUTER MEMBRANES)	ENDOPLASMIC RETICULUM	*E. COLI* BACTERIUM
Cholesterol	17	23	22	3	6	0
Phosphatidylethanolamine	7	18	15	25	17	70
Phosphatidylserine	4	7	9	2	5	trace
Phosphatidylcholine	24	17	10	39	40	0
Sphingomyelin	19	18	8	0	5	0
Glycolipids	7	3	28	trace	trace	0
Others	22	13	8	21	27	30

Table 10-1

.

Approximate Lipid Compositions of Different Cell Membranes

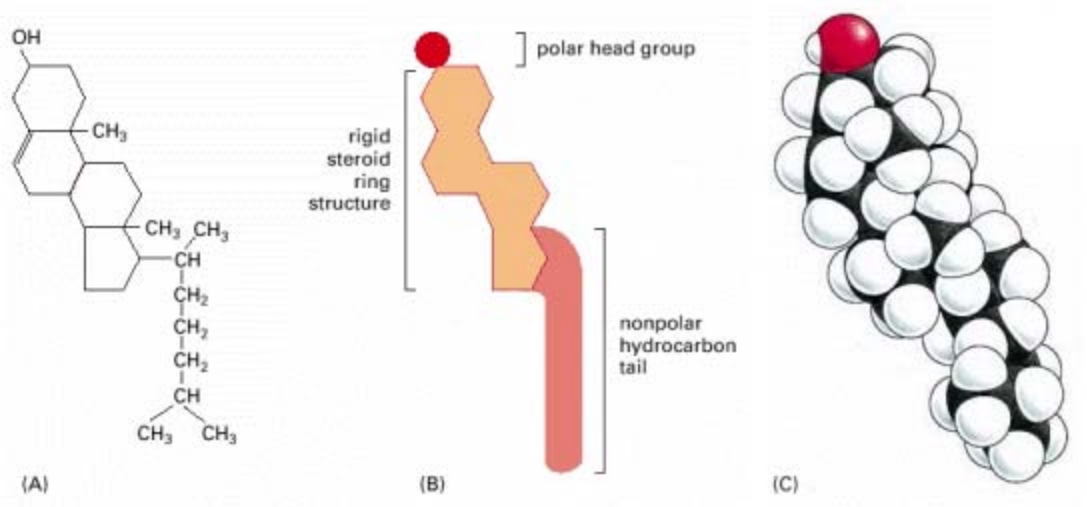

Figure 10-10
. **The structure of cholesterol**
Cholesterol is represented (A) by a formula, (B) by a schematic drawing, and (C) as a space-filling model.

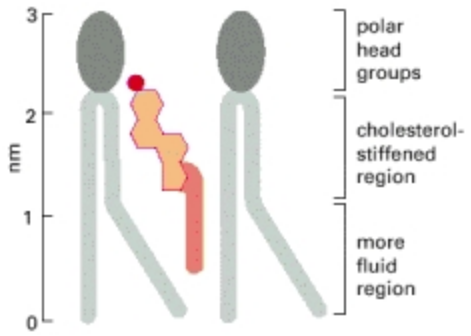

Figure 10-11
. **Cholesterol in a lipid bilayer**
Schematic drawing of a cholesterol molecule interacting with two phospholipid molecules in one monolayer of a lipid bilayer.

http://www.ncbi.nlm.nih.gov/bookshelf/br.fcgi?book=mboc4&part=A1864&rendertype=figure&id=A1876

http://www.ncbi.nlm.nih.gov/bookshelf/br.fcgi?book=mboc4&part=A1864&rendertype=figure&id=A1877

Head group

Linkage

Tail group

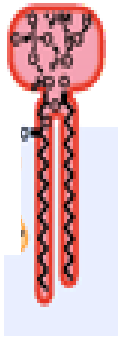

Saturated
alkyl chains

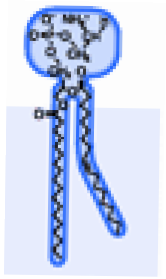

Unsaturated
alkyl chains

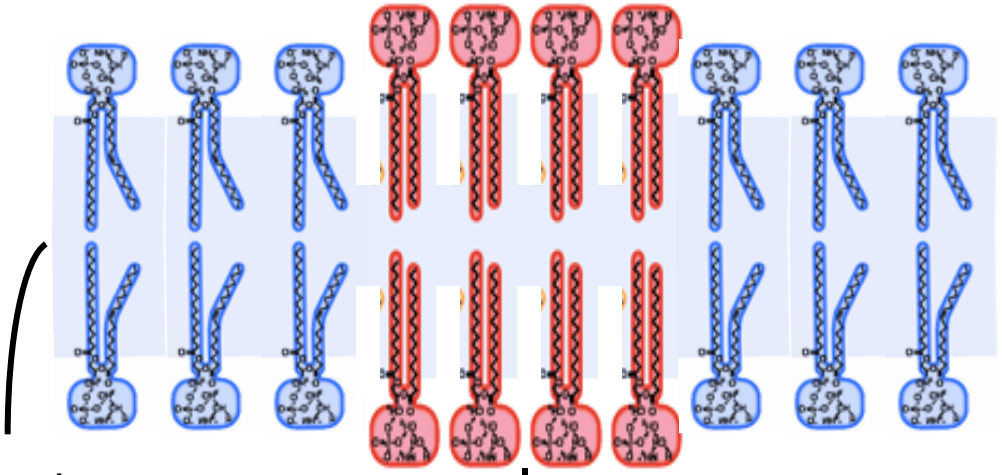

“fluid” phase

“gel” or liquid crystalline phase
densely packed
more ordered
~10-15 Å higher

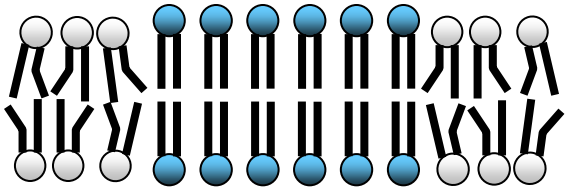

gel domain

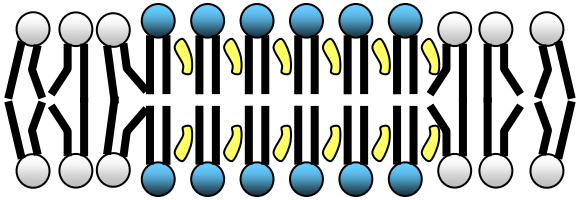

liquid-ordered domain
“lipid raft”

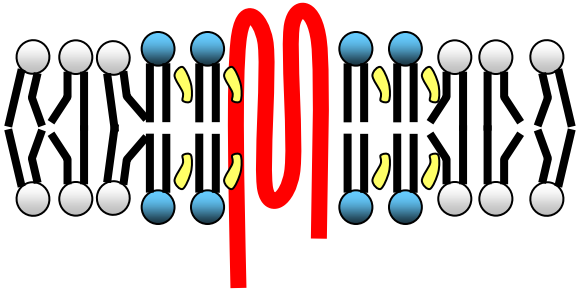

partitioning of
membrane proteins

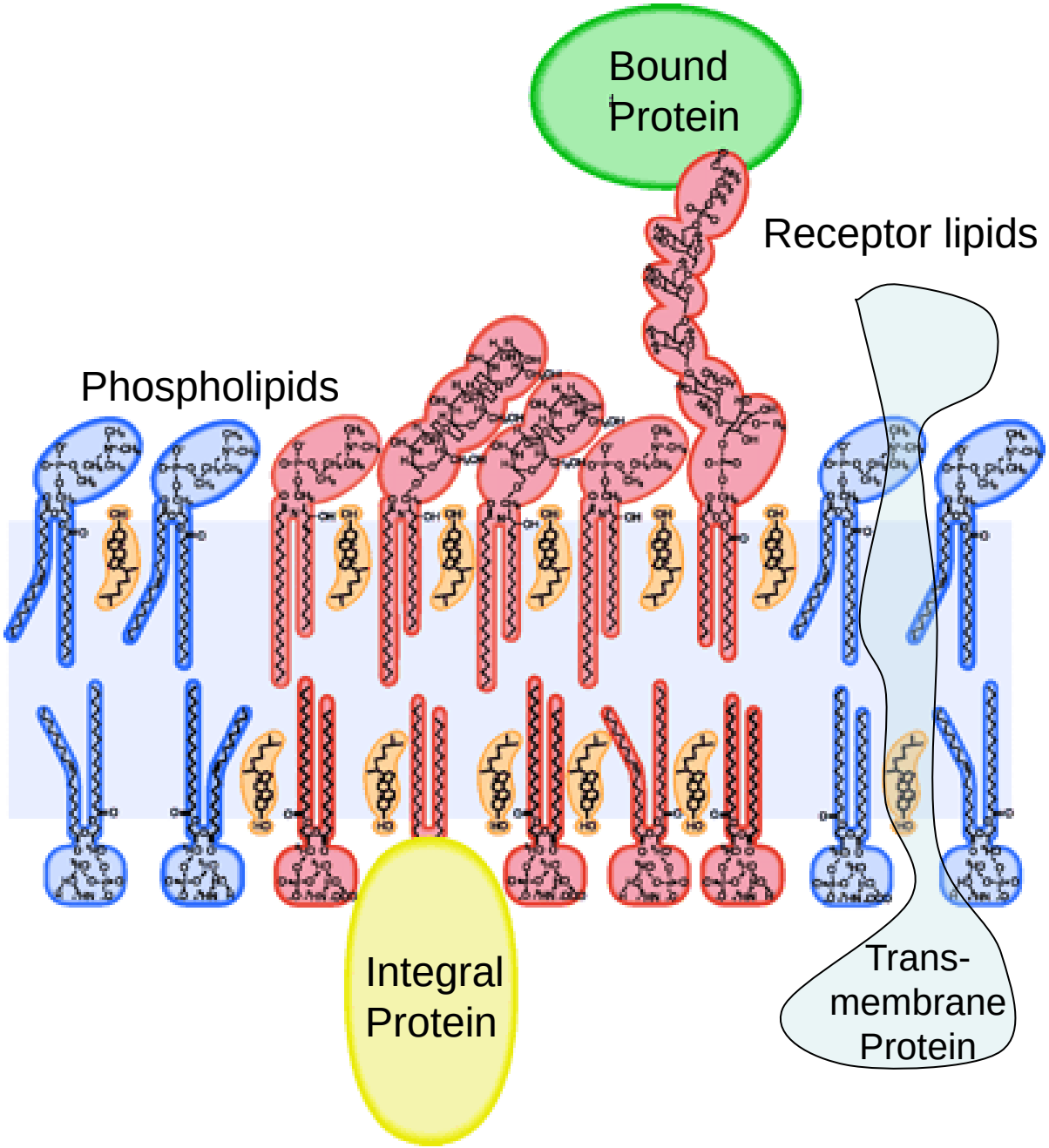

Simons, *Science* **290** 1721 (2000)

Modern view of the membrane

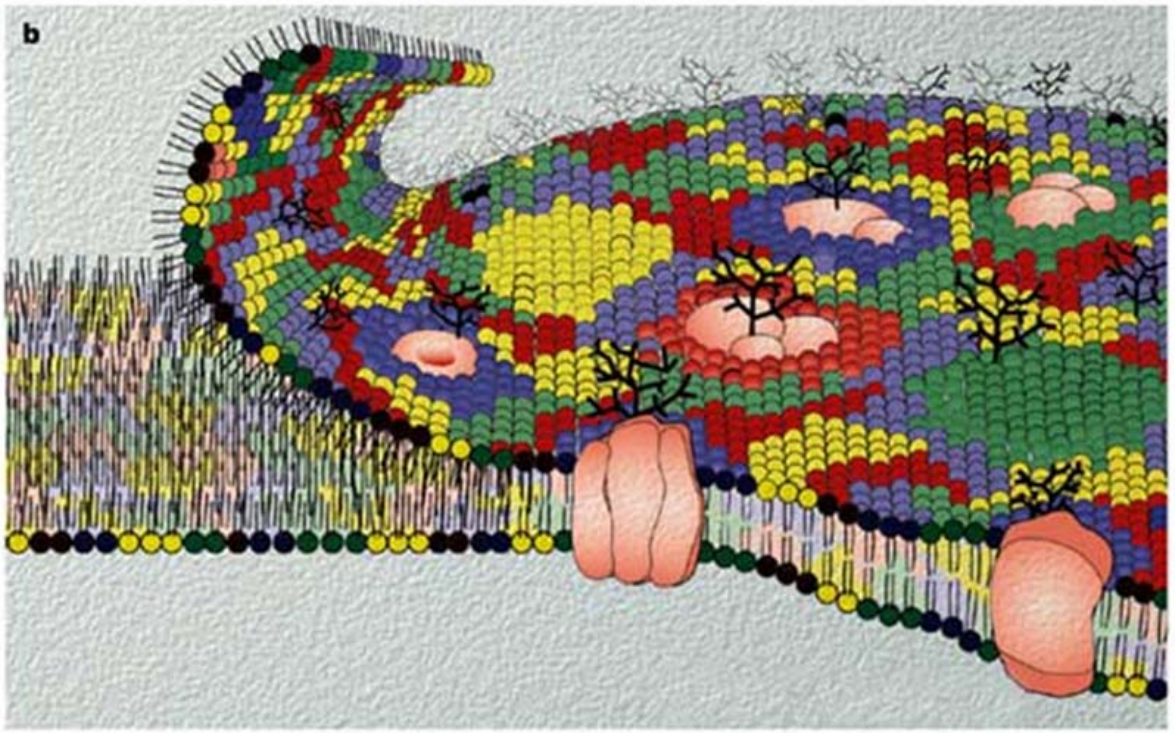

Nature Reviews | Molecular Cell Biology

1-palmitoyl-2-oleoyl-sn-glycero-3-phosphocholine
(POPC)

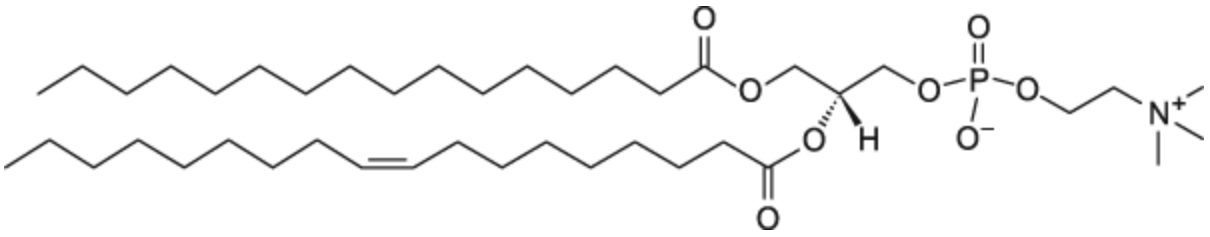

N-dinitrophenyl-aminocaproyl phosphatidylethanolamine
(16:0 DNP-Cap PE)

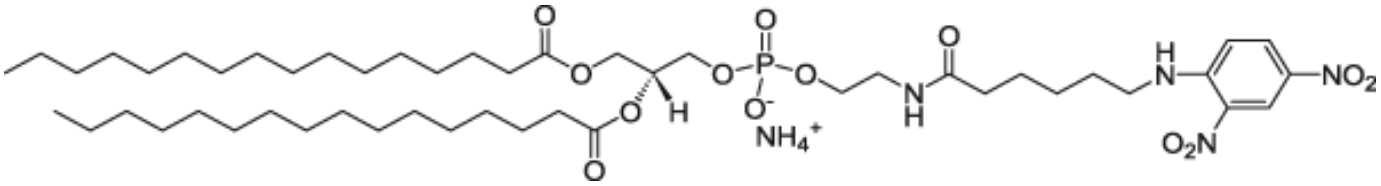

What is the meaning of "sn" in the lipid name?
Answer
From "Nomenclature of Lipids", IUPAC-IUB Commission on Biochemical Nomenclature (CBN) (www.chem.qmul.ac.uk/iupac/lipid)

Lip-1.13. Stereospecific Numbering. In order to designate the configuration of glycerol derivatives, the carbon atoms of glycerol are numbered stereospecifically. The carbon atom that appears on top in that Fischer projection that shows a vertical carbon chain with the hydroxyl group at carbon-2 to the left is designated as C-1. To differentiate such numbering from conventional numbering conveying no steric information, the prefix 'sn' (for stereospecifically numbered) is used.

Mast Cell Signaling: the cornerstone of allergic inflammation

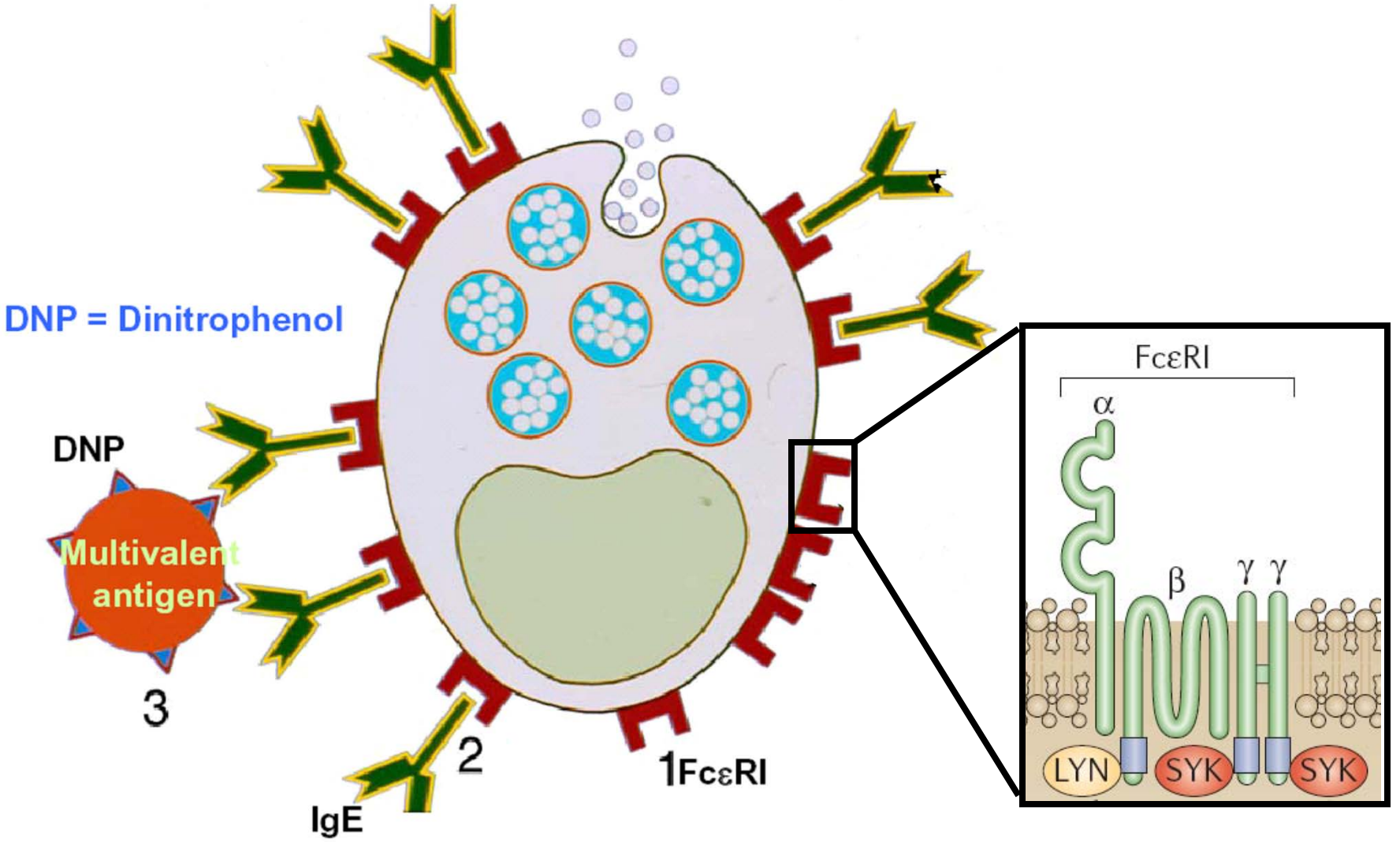

Gilfillan, 2006 *Nat. Rev. Immunol*

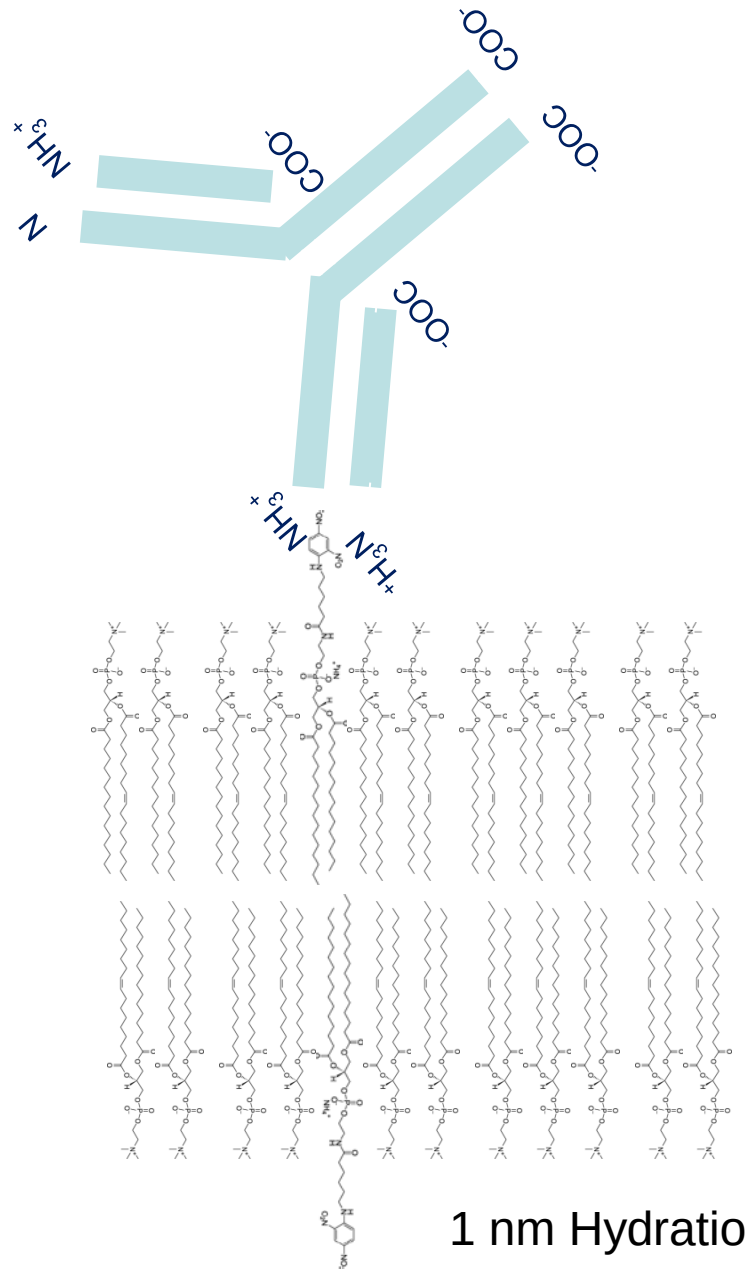

1 nm Hydration Layer

Lateral mobility of proteins in liquid membranes revisited

Y. Gambin*†, R. Lopez-Esparza*, M. Reffay*, E. Sierecki‡, N. S. Gov§, M. Genest¶, R. S. Hodges¶, and W. Urbach*

*Laboratoire de Physique Statistique de l'Ecole Normale Supérieure, Unité Mixte de Recherche 8550, Centre National de la Recherche Scientifique–Université Paris 6, 24 Rue Lhomond, 75005 Paris, France; ‡Synthèse et Structure de Molécules d'Intérêt Pharmacologique, Unité Mixte de Recherche 8638, Centre National de la Recherche Scientifique–Université Paris 5, 4 Avenue de l'Observatoire, 75006 Paris, France; §Department of Chemical Physics, The Weizmann Institute of Science, Rehovot 76100, Israel; and ¶Department of Biochemistry and Molecular Genetics, University of Colorado, Denver, CO 80045

The biological function of transmembrane proteins is closely related to their insertion, which has most often been studied through their lateral mobility. For >30 years, it has been thought that hardly any information on the size of the diffusing object can be extracted from such experiments. Indeed, the hydrodynamic model developed by Saffman and Delbrück predicts a weak, logarithmic dependence of the diffusion coefficient D with the radius R of the protein. Despite widespread use, its validity has never been thoroughly investigated. To check this model, we measured the diffusion coefficients of various peptides and transmembrane proteins, incorporated into giant unilamellar vesicles of 1-stearoyl-2-oleoyl-*sn*-glycero-3-phosphocholine (SOPC) or in model bilayers of tunable thickness. We show in this work that, for several integral proteins spanning a large range of sizes, the diffusion coefficient is strongly linked to the protein dimensions. A heuristic model results in a Stokes-like expression for D, ($D \propto 1/R$), which fits literature data as well as ours. Diffusion measurement is then a fast and fruitful method; it allows determining the oligomerization degree of proteins or studying lipid–protein and protein–protein interactions within bilayers.

www.pnas.org/cgi/doi/10.1073/pnas.0511026103

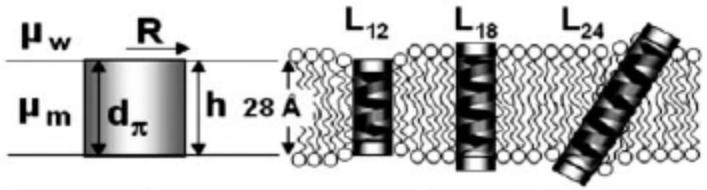

Name & Symbol	Sequence	d_π	D (μm²/s) SOPC
L_{12} ●	AKK-$(L)_{12}$-GKK-Fitc	19 Å	0.29 ±0.02
L_{18} □	AKK-$(L)_{18}$-GKK-Fitc	28 Å	0.31 ±0.02
L_{24} ◆	AKK-$(L)_{24}$-GKK-Fitc	37 Å	0.21 ±0.01

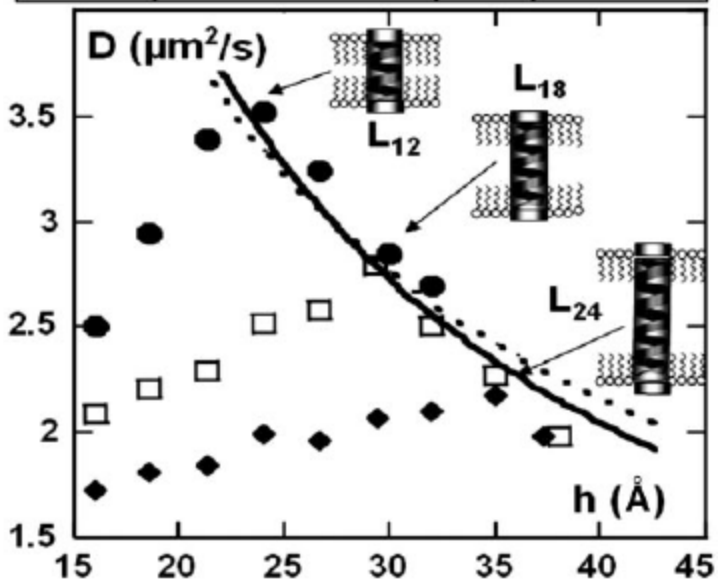

Fig. 1. Peptides used and their D variations versus bilayer thickness h. (*Top*) The parameters used in the Saffman–Delbrück model (Eq. **1**), in the case of peptides diffusing in a giant unilamellar vesicle (GUV) made of SOPC. (*Middle*) A summary of the properties of the peptides used, their sequences, and their hydrophobic length d_π. The right-hand column gives the measured diffusion coefficient of these peptides in single GUVs. The diffusion coefficient was determined by using evanescent fluorescence recovery after pattern photobleaching technique. The data are typically averaged >200 vesicles. (*Bottom*) The variation of the diffusion due to the swelling of the $C_{12}E_5$ bilayer for the three analog peptides L_{12} (●), L_{18} (□), and L_{24} (◆). For each peptide, five sets of experiments allowed us to obtain average values with a reproducibility of >5% (the symbol size). The dotted line is the fit with the Saffman–Delbrück model (Eq. **1**), using only one adjustable parameter, μ_m. The radius was taken as 5.5 Å and the viscosity of water as 0.01 P, leading to $\mu_m = 2.94$ P. The solid line represents a simple $1/h$ dependence. Note that the relative D variations are the same in $C_{12}E_5$ bilayers and in SOPC membranes: for $h = 28$ Å, L_{24} diffuses 30% slower than L_{18}; L_{12} and L_{18} have similar mobilities.

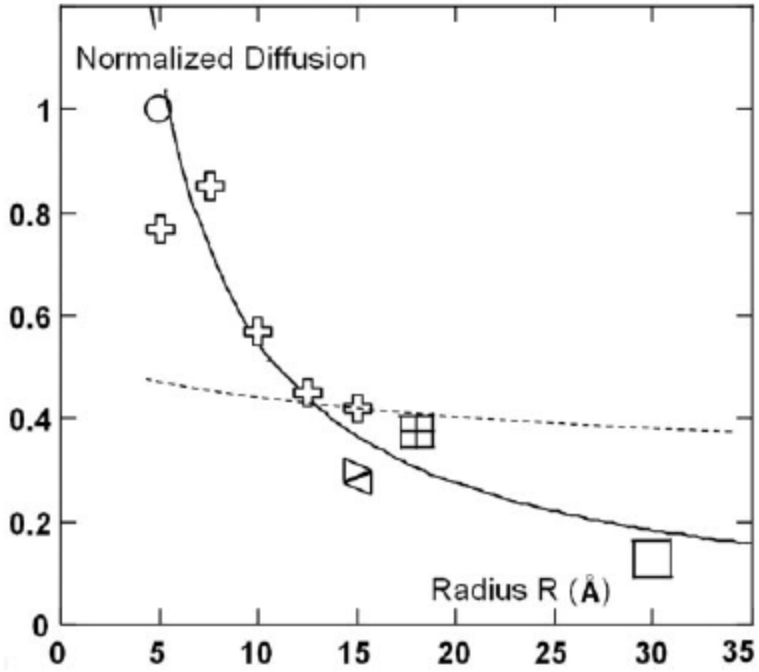

Fig. 2. Normalized diffusion coefficient (D/D_{lipid}) vs. peptide radius R in lipid bilayers. Crosses correspond respectively from the left to monomers, dimers, trimers, tetramers, and hexamers of transmembrane peptides (15). The square symbols at R = 15, 18, and 30 Å correspond, respectively, to acetylcholine receptor (AChR), BR, and SR-ATPase (16). The solid line is a $1/R$ fit, and the dashed line represents the prediction of Saffman's model, using $h = 28$ Å, $\mu_m = 1.75$ P, and $\mu_w = 1$ cP as in ref 15.

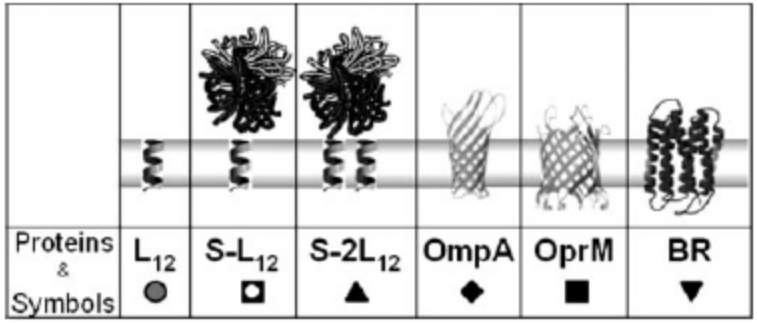

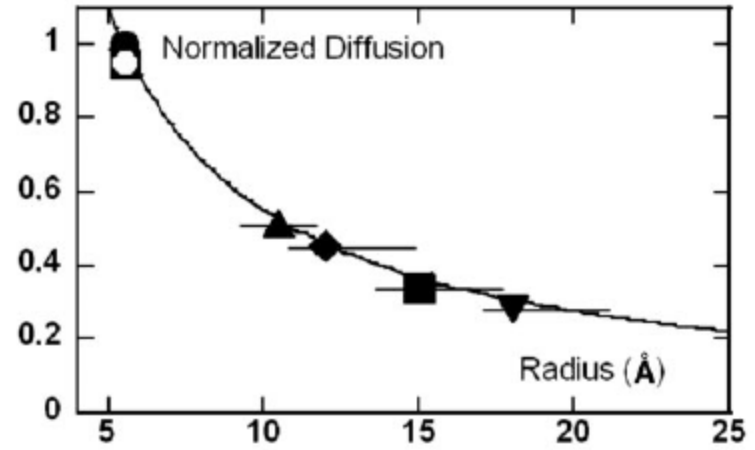

Radius	5.5Å	5.5 Å	10.5 Å	11 Å	14 Å	18 Å
D	D_0	0.97 D_0	0.51 D_0	0.45 D_0	0.34 D_0	0.26 D_0
$R_{Saffman}$	5.5Å	6.7 Å	138 Å	160 Å	320 Å	520 Å
$R_{(1/R)}$	5.5Å	5.7 Å	10.8 Å	12.2 Å	16.2 Å	21.1 Å

Fig. 3. Normalized diffusion coefficient ($D/D_{L_{12}}$) vs. peptide radius R, in $C_{12}E_5$ bilayers. The formation of streptavidin-peptide assemblies is described in *Materials and Methods*. To avoid possible denaturation, the transmembrane proteins are embedded in dodecane-free membranes. The hydrophobic mismatch between protein height and bilayer thickness creates a local deformation. As discussed in *Materials and Methods*, this effect leads to a large uncertainty in the effective radius of the protein, represented by the horizontal bars in the plot. The diffusion coefficients are normalized by the diffusion of the L_{12} peptide ($R_{L_{12}} = 5.5$ Å $\sim R_{SOPC}$), extrapolated to the thickness of a dry bilayer in Fig. 1 ($D_0 = 4.8 \pm 0.2\ \mu m^2/s$). From the measured D values and Eq. **1**, one can estimate the corresponding

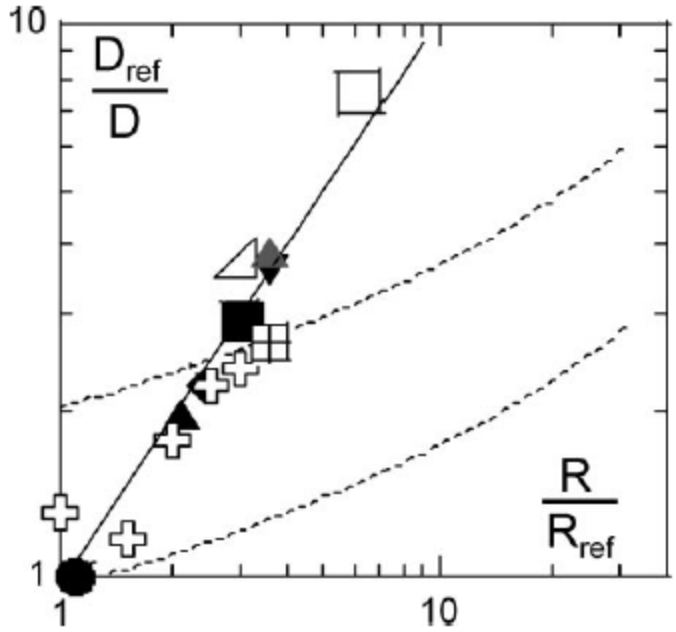

Fig. 4. Normalized inverse diffusion coefficient D_{ref}/D vs. object radius R/R_{ref}, (open symbols are data gathered from the literature, and filled symbols are from this work). For peptide assemblies and proteins in $C_{12}E_5$ bilayers (filled symbols as in Fig. 3), the peptide L_{12} serves as reference: $D_{ref}/D = D_{L12}/D$; the BR in SOPC (gray triangle) is compared with the L_{18} peptide: $D_{ref}/D = D_{L18}/D$. As in Fig. 2, for oligomers of peptides (crosses), acetylcholine receptor (AChR), BR, and SR-ATPase (squares), the lipid diffusion serves as reference. The solid line is a power-law regression leading to $D_{ref}/D \propto R^{1.04}$; for comparison, the dashed line represents the prediction of the Saffman–Delbrück model (Eq. **1**) (upper line, same as in Fig. 3, and lower fit as in Fig. 2).

Our experimental results, as well as published data, indicate that the diffusion coefficient is inversely proportional to the radius R of the diffusing object (Fig. 4) and to the thickness h of the membrane (Fig. 1). These observations suggest a heuristic Stokes–Einstein-like expression

$$D = \frac{k_B T \lambda}{4\pi \mu_m h \cdot R}, \qquad [2]$$

where a characteristic length, λ, is introduced for dimensional reasons.